

## COPPER OXIDE CATHODES FOR LITHIUM ORGANIC ELECTROLYTE BATTERIES

P PODHAJECKY\* and B SCROSATI

*Dipartimento di Chimica, University of Rome (Italy)*

(Received March 27, 1985, in revised form December 6, 1985)

### Summary

The discharge characteristics of the Li/CuO battery with various types of cupric oxide cathodes have been investigated. The results reveal that the morphology of the cathode material plays a very important role in the discharge performance of the battery

---

### Introduction

Cupric oxide is a very good cathodic material for lithium organic electrolyte batteries. Its high specific capacity (*i.e.*, 0.67 A h/g and 4.26 A h/cm<sup>3</sup>) makes it ideal for the development of batteries with high volumetric energy density and having a voltage (around 1.5 V) compatible with that of the commonly used dry cells. Various types of Li/CuO batteries have been characterized and are already being produced, mainly for the electronic market [1].

Although the Li/CuO system has been examined by various authors [2 - 6], there are still some uncertainties on the electrochemical discharge mechanism. The definition of the cell reaction is important for the correct evaluation of the basic properties of a power source.

The electrochemical properties of differently prepared CuO samples have been examined previously [5]. No correlation, however, was found between the surface area and the electrochemical properties, this possibly being associated with the presence of impurities in the samples. In this work particular care was therefore devoted to the preparation of CuO samples of different morphology, using methods which gave promise of excluding any possible contamination.

---

\*On leave from J Heyrovsky Institute of Physical Chemistry and Electrochemistry of the Czechoslovak Academy of Sciences, Prague

## Experimental

Various types of CuO samples were used for the electrochemical tests in lithium cells having a 1 M solution of lithium perchlorate ( $\text{LiClO}_4$ ) in propylene carbonate (PC) as the electrolyte.

The first four samples were prepared from the same starting material, CuH, following the general procedure described by Remy [7]. This procedure appeared to us to be more suitable, in view of the need to exclude contamination, than that based on precipitation from alkaline media.

Copper oxide samples having different morphology were obtained by varying the preparation conditions. The decomposition of CuH with water or a copper salt solution at elevated temperature gave copper and, in part,  $\text{Cu}_2\text{O}$ , especially in the presence of nitrates. The final CuO samples were obtained by heating at 400 °C in air for 3 h and then in an oxygen atmosphere for a further 3 h.

We have considered six different samples having the following basic characteristics (see Table 1)

*Sample 1* CuH was decomposed by drying under vacuum and annealing at 80 °C for 1 h

*Sample 2* CuH was suspended in boiling water for 2 h. The product was then washed and dried.

*Sample 3* The preparation was similar to that of sample 2, boiling CuH in a 1 M  $\text{CuSO}_4$  aqueous solution for 2 h and drying the final compound.

*Sample 4* Again, the preparation involved boiling CuH, in this case in a 1 M  $\text{CuNO}_3$  solution, and drying the final compound.

TABLE 1

Characteristics and properties of various samples of cupric oxide as cathodes in lithium, organic electrolyte cells

Sample no	Max particle size ( $\mu\text{m}$ )	BET surface area ( $\text{m}^2 \text{g}^{-1}$ )	$C_1/C_t$ (%)	$C_{\text{exp}}/C_t$ (%)
1	2	3.98	10	80
2	3	0.88	5	85
3	10	0.80	4	75
4	20	0.41	3	40
5	—	1.20	9	80
6	—	7.33	14	55

$C_t$  = Total capacity (Theoretical for the reaction  $\text{Cu}^{2+} + 2\text{e}^- = \text{Cu}$ )

$C_1$  = Capacity developed in the first step of the discharge

$C_{\text{exp}}$  = Experimental capacity obtained to 0.9 V cut-off voltage

**Sample 5** This sample was prepared by oxidation of commercial  $\text{Cu}_2\text{O}$  in air (30 min) and in oxygen (30 min) at 400 °C.

**Sample 6** This sample was commercial CuO (Merck reagent grade), used for comparison purposes.

The electrolyte solution was prepared from the components after purification by recrystallization under vacuum ( $\text{LiClO}_4$ ) and by fractional distillation (PC).

A two-electrode laboratory cell was used for the electrochemical tests. Cupric oxide was mixed with copper in a 2:1 weight ratio and about 50 to 60 mg of this mixture was pressed directly onto a stainless steel current collector to form a 1.3 cm<sup>2</sup> cathodic pellet. This pellet was separated from the lithium anode by glass-fiber disks soaked with the  $\text{LiClO}_4$ -PC electrolyte.

For the discharge evaluation of the best selected CuO sample, crimp-sealed button cells were used with a 1 M solution of  $\text{LiClO}_4$  in a propylene carbonate-dimethoxyethane (PC-DME) solvent mixture as the electrolyte.

The discharge curves were recorded by a computer-controlled data acquisition system whose characteristics are described in detail elsewhere [8].

The current-voltage curves were obtained using a galvanostat driven by a function generator for controlling the current scans and a computer for storing the potential data. The current was loaded as a linear function of time in the range -1 mA to +1 mA with a sweep rate of 0.25 mA min<sup>-1</sup>. In these experiments, the same two-electrode system cell was used as in the other measurements. In fact, the polarization of the Li anode is negligible at the given current densities and the quantity of Li was in large excess as compared with the cathode capacity.

## Results and discussion

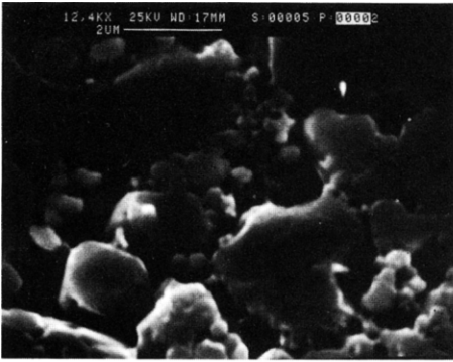
### *Characteristics of the CuO samples*

As already mentioned, the morphology of the final CuO samples depends on the conditions of preparation. The particles of samples 1, 5, and 6 are very small and not distinguishable by scanning electron microscopy. Differences in the morphology of the other samples are observable in Fig. 1. Sample 2 (Fig. 1(A)) consists of regularly-shaped (approximately 3  $\mu\text{m}$ ) particles. Sample 3 (Fig. 1(B)) has irregular particles having an average size greater than 10  $\mu\text{m}$ . Finally, sample 4 (Fig. 1(C)) has randomly-shaped particles with an average size greater than 20  $\mu\text{m}$ .

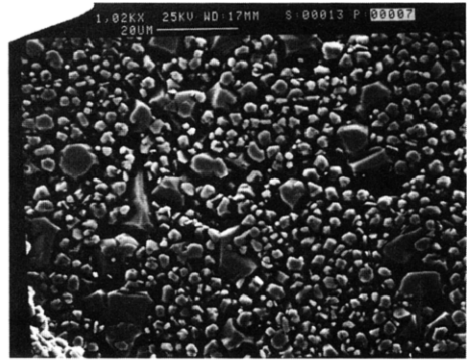
The differences in particle size of the samples result in differences in the discharge behaviour, as indicated below.

### *Discharge mechanism*

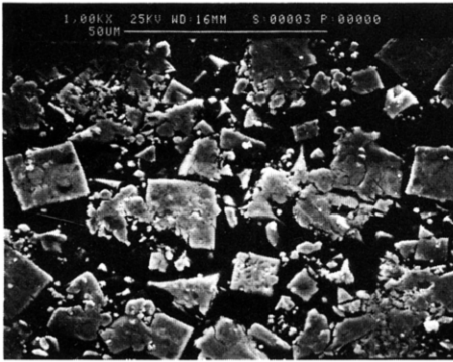
Figures 2 and 3 show typical discharge curves of Li/CuO cells using the six CuO samples. The general discharge trend is similar for all samples,



(a)



(b)



(c)

**Fig 1** Scanning electron microscope (SEM) photographs of CuO samples (a), Sample 2, (b) sample 3, (c) sample 4

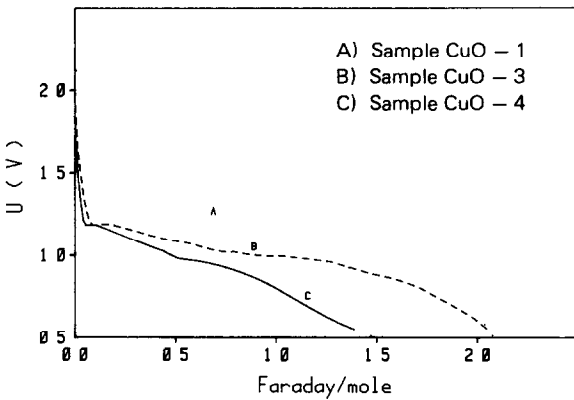


**Fig 2** Typical discharge curves at 0.5 mA and at 20 °C of Li/CuO cells using CuO samples nos 1, 3, and 4

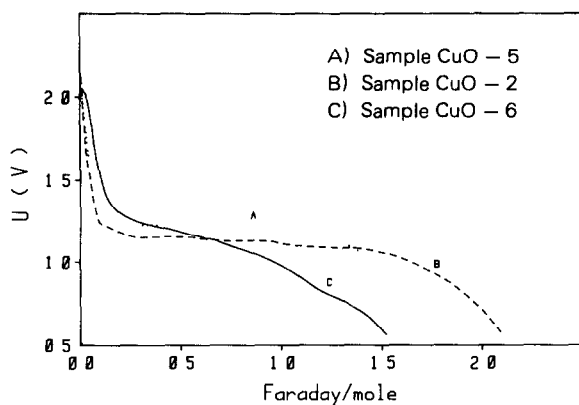


Fig 3 Typical discharge curves at 0.5 mA and at 20 °C of Li/CuO cells using CuO samples nos 2, 5, and 6

involving a first step between 2.3 V and 1.3 V, followed by an extended plateau around 1.3 V. Within this general trend, some specific differences between the six cells are seen, especially in relation to the extent of the first step and to the voltage stability of the second low voltage plateau.

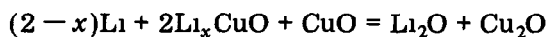
The general discharge trend of the Li/CuO system has been discussed by Bates and Jumel [1] who reported that at temperatures around 70 °C the low voltage discharge evolved along two plateaux, the first at about 1.6 V and the second at about 1.4 V. On the basis of these observations, the authors concluded that the discharge mechanism of the Li/CuO cell may first involve the insertion of lithium into the CuO lattice:



followed by the reduction of CuO according to the scheme



or:



Reaction (1) involves  $x$  electrons per CuO mole while reactions (2) and (3) involve  $(2-x)$  electrons per CuO mole.

The above reaction scheme seems to be confirmed by the results obtained in this work. The discharge curves involve 100% theoretical capacity ( $C_t$ ) for a two-electron reaction. Figures 2 and 3 show that the extent of the first step ( $C_1$ ) decreases from sample 1 to sample 4, *i.e.*, with decreasing surface area of the cathodic material. This would be consistent with, but not exclusive to, reaction (1) being an insertion process. Such a type of process is further suggested, however, if this part of the discharge is reversible and, in fact, we have been able to cycle a Li/CuO (sample 1) cell several

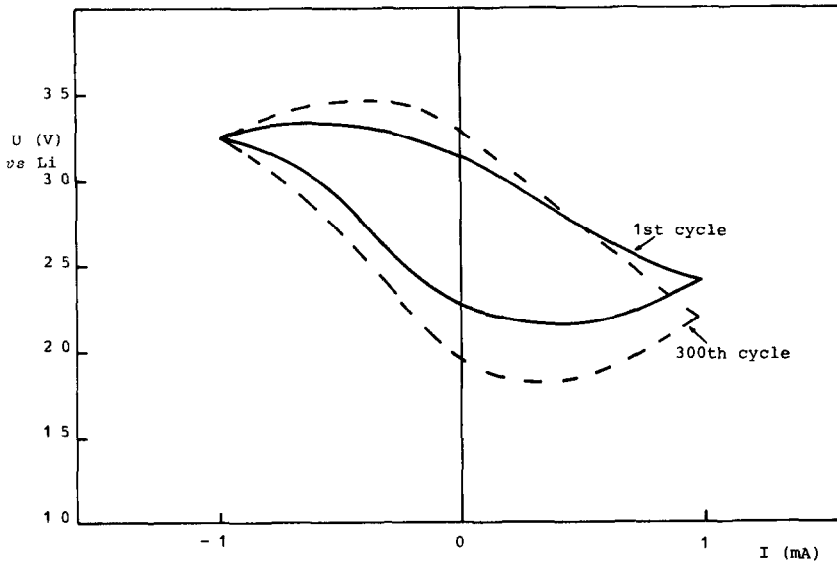


Fig 4 Current-voltage curves of the CuO electrode at the initial state of discharge Sweep rate  $0.25 \text{ mA min}^{-1}$  Electrode surface  $1.3 \text{ cm}^2$

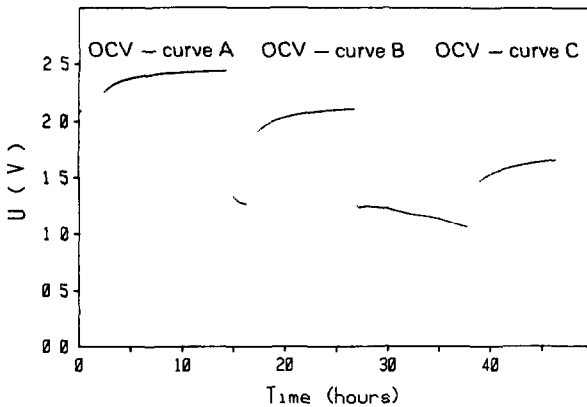


Fig 5 Voltage recovery of the Li/CuO cell at different states of discharge (A) First discharge step, (B) second discharge step, (C) after 50% of  $C_t$  Discharge current  $0.5 \text{ mA}$  Temperature  $25^\circ \text{C}$  CuO sample no 1

times over the initial stage of discharge. A typical cyclic voltammogram involving 0.32% of the total capacity is shown in Fig. 4. Voltammograms of this type could be repeated more than 300 times under an oxygen and water controlled atmosphere. The total charge passed was about 100% of the theoretical capacity at potentials higher than 1.8 V. This definitely shows that the initial portion of the discharge curve is not solely due to the reaction of adsorbed water and/or oxygen, which can be considered to be irreversible.

Figure 5 shows the voltage recovery after different states of discharge of the Li/CuO cell. It can be seen that the open circuit voltage (OCV)

reached different levels with different kinetics according to the discharge state. If the current is switched off during the first insertion step, the OCV quickly reaches 2.5 V (curve A). When the discharge is interrupted at the low voltage plateau, the OCV rises more slowly, approaching 2.2 V at the beginning of the plateau (curve B) and 1.8 V after a 50% discharge (curve C). These results point to slow diffusion in the copper oxide and to the presence of  $\text{Cu}_2\text{O}$  when 50% of  $C_t$  is reached.

The diffusion of  $\text{Li}^+$  ions into  $\text{CuO}$  particles is certainly slow. Hence, the intercalation reaction proceeds mainly at the surface. As soon as the capacity of the surface layer is exhausted, the course of the reaction changes from reaction (1) to reactions (2) and (3) and the cell voltage reaches a plateau at 1.2 - 1.5 V. The cell voltage continues to be influenced by reaction (1), however, *via*, by the diffusion of  $\text{Li}^+$  ions into the  $\text{CuO}$  particles, thus explaining the different values of the voltage plateau for cells using samples 2 and 5 (Fig. 3). Sample 6, however, having a relatively large surface area, does not give a comparable discharge capacity at the current rates used. Measurement of the diffusion coefficient of  $\text{Li}^+$  ions in the solid phase could possibly elucidate this phenomenon. These measurements will be the subject of further work.

The reaction mechanism and sequence proposed above seem to be confirmed by ESCA analysis performed on the surface of two  $\text{CuO}$  cathodes at different stages of discharge, namely, after  $0.08 \text{ F mole}^{-1}$  and after  $0.3 \text{ F mole}^{-1}$ , respectively.

The curve fitting, performed on the  $\text{Cu}_{2p_{3/2}}$  signal shows, in both cases, an intense peak (about 75 to 80% of the entire signal) which may be ascribed to  $\text{Cu}_2\text{O}$  and a weaker peak (20 - 25% of the total intensity) at higher bonding energy, which is typical of the  $\text{CuO}$  species.

The fact that  $\text{Cu}$  appears in both samples with two oxidation states may, indeed, support the hypothesis of the formation of a compound of the  $\text{Li}_x\text{CuO}$  type. In fact, one may consider, by analogy, the typical spectrum of a bronze such as  $\text{Na}_x\text{WO}_3$ , where a series of signals associated with discrete oxidation states of tungsten ( $\text{W}^{+4}$ ,  $\text{W}^{+5}$ ,  $\text{W}^{+6}$ ) are present [9].

### Cell performance

Figure 6 shows discharge curves of the  $\text{Li}/\text{CuO}$  (sample 1) cell at various temperatures. The two plateaux described by Bates and Jumel [1] are clearly distinguishable.

The typical discharge curves illustrated in Figs. 2 and 3 show that, in general, samples 1 and 2 have the same discharge trend, even if the latter, which has an optimized particle size, presents the best performance. This type of  $\text{CuO}$  was therefore selected for the battery tests.

Figure 7 shows the initial trend of discharge curves of a button type  $\text{Li}/\text{CuO}$  battery. It may be seen that the first step is limited in extent and that the discharge develops with a very good voltage stability around 1.4 V, confirming the good capabilities of the  $\text{Li}/\text{CuO}$  system.

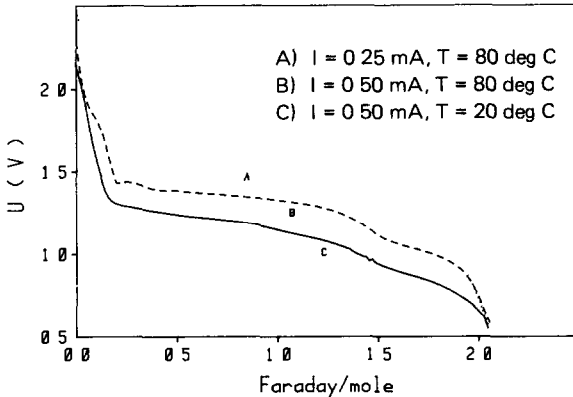


Fig 6 Discharge curves of the Li/CuO (sample no 1) at various currents and at various temperatures

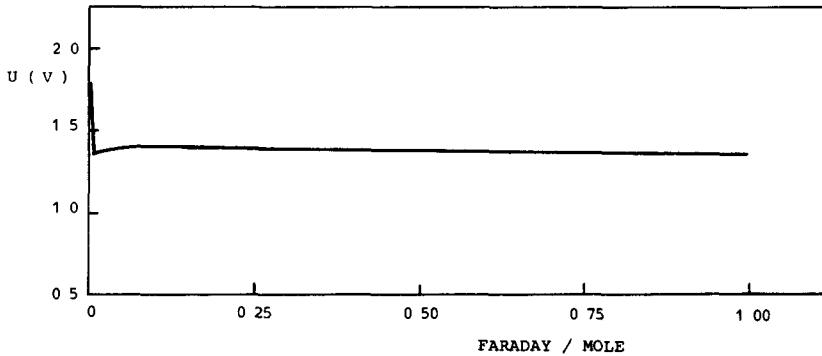


Fig 7 Initial discharge curve at 0.25 mA of a Li/CuO button type battery at room temperature Battery dimensions  $11.5 \times 4$  mm

## Conclusions

The morphology of the particles plays an important role in the selection of the most suitable CuO cathode material for lithium, organic electrolyte batteries. To restrict the initial portion of the discharge curve, it is necessary to choose an optimum particle size, *i.e.*, about  $1 - 3 \mu\text{m}$  with about  $1 \text{ m}^2 \text{ g}^{-1}$  specific area. Larger particles give a low utilization of the available capacity.

## Acknowledgements

We thank Dr L. Sabbatini of the University of Bari for the ESCA measurements. One of us (P.P.) is grateful to the Italian Government for a Fellowship. This work was carried out with the financial support of the Ministero Pubblica Istruzione.



## References

- 1 R Bates and Y Jumel, in J P Gabano (ed ), *Lithium Batteries*, Academic Press, London, 1983, p 73
- 2 J P Gabano, *US Pat* 3,542,602 (1967)
- 3 G Lehmann, G Gerbier, A Brych and J P Gabano, in D H Collins (ed ), *Power Sources*, 5, Academic Press, London, 1975, p 695
- 4 L Takashi, T Yoshinoro, N Joji and O Hiromichi, *J Power Sources*, 5 (1980) 99
- 5 P Podhajecky, B Klapste, J Mrha, R Moshtev, V Manev and A Nasalevska, *J Power Sources*, 14 (1985) 269
- 6 P Novak, B Klapste and P Podhajecky, *J Power Sources*, 15 (1985) 101
- 7 H Remy, in *Lehrbuch der Anorganischen Chemie*, Akademische Verlagsgesellschaft, Geest und Portig, Leipzig, 1954
- 8 F Bonino and B Scrosati, to be published
- 9 B A De Angelis and M Schiavello, *Chem Phys Lett* , 58 (1978) 249